Polyhedral Topological Crystals

Masakatsu Tsubota,[*,†] Katsuhiko Inagaki,[‡] Toru Matsuura,[¶] and Satoshi Tanda[†,§]

Department of Applied Physics, Hokkaido University,Sapporo 060-8628, Japan, Department of Physics, Asahikawa Medical University, Asahikawa 078-8510, Japan, Creative Research Institute, Research Department, Hokkaido University, Sapporo 001-0021, Japan, and Center of Education and Research for Topological Science and Technology, Hokkaido University, Sapporo 060-8628, Japan

E-mail: tsubota@eng.hokudai.ac.jp

Phone: +81 (11)706 7293. Fax: +81 (11)706 7293

Abstract

We synthesized micrometer-scale polyhedral ring-crystals of TaS_3, by the chemical vapor transportation method. The polyhedral ring-crystals are closed-loop crystals with several vertices. We investigated the crystallinity and flatness of the facets by the electron backscatter diffraction pattern technique, and revealed that the orientation of crystal axis changes abruptly at several points. Observing the size of the crystals, we found a new phase of topological crystals, and proposed a phase diagram of ring-polyhedral crystals in terms of radius and thickness. We proposed the mechanism of polygonization in which the vertices of the polyhedral crystals are formed of concentrated dislocations caused by the distance-dependent interaction between them.

[*]To whom correspondence should be addressed
[†]Department of Applied Physics, Hokkaido University
[‡]Department of Physics, Asahikawa Medical University
[¶]Creative Research Institute, Research Department, Hokkaido University
[§]Center of Education and Research for Topological Science and Technology, Hokkaido University

Introduction

Recently, there has been increasing interest in loop nano-structures and micro-structures.[1–3] The theoretical and experimental attention has been paid to the crystal of these structures.[4–7] Topological crystals were discovered in 2000[8] and have been researched. First, an $NbSe_3$ ring crystal was synthesized together with whisker crystals. Next, other topological crystals (Möbius strip, figure-of-eight, and Hopf-link shaped crystals) were discovered,[9,10] and then topological crystals of other compounds ($TaSe_3$,[11] TaS_3[12] and NbS_3[13]) were discovered. Crystal topology broke through a new stage of understanding of physical phenomena.[12,14,15]

The topological crystals are conceptually different from conventional crystals. A crystal is constructed by the infinite repetition of atoms, as shown in Figure 1 (LEFT). Then the conventional crystal displays discrete translational and rotational symmetries, and the crystal lattices can be mapped into themselves by the translational symmetry or by various other symmetry operations. On the other hand, the topological crystal does not display discrete translational or rotational symmetries, because the orientation of the crystal axes is smoothly changed. It also indicates that the distribution of the dislocations/disclinations introduced in the topological crystals [as shown in Figure 1 (RIGHT)] must be smooth.[16,17] When the topological crystal needs to be bent, geometrical frustration is relaxed by inclusion of the edge dislocation, and other kinds of dislocation, such as screw and mixed dislocation are not necessary to be considered.[18–20] However, the interplay between the global topology of the crystals and the distribution of dislocations/disclinations has been unclear yet.

In this paper, we report a new type of topological crystals having several vertices in tantalum trisulfied (TaS_3) system. Using the electron backscatter diffraction technique, we confirmed the crystallinity and flatness of the facets in the ring and polyhedral crystals, and then revealed that the orientation of crystal axes on the polyhedral ring crystals changes abruptly at several points. To reveal growth mechanism of the polyhedral crystals, we investigated several topological crystals about the radius and width. From the radius-width diagram, we propose a phase diagram of smooth-polyhedral topological crystals, based on that predicted by Hayashi *et al*.[21]

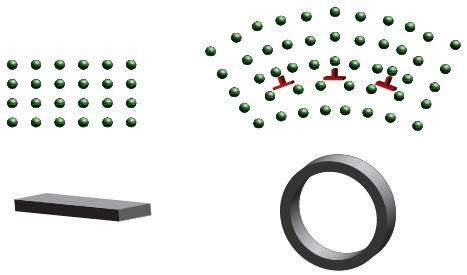

Figure 1: Structure of (LEFT) the needle-shaped crystal and (RIGHT) the ring-shaped crystal. Resulting with the expansion and contraction, the dislocations are generated ($\perp$ symbols).

Experimental Methods

The polyhedral ring crystal samples of TaS_3 were synthesized by the chemical vapor transport (CVT) method. We enclosed starting materials (a tantalum wire and sulfur powder with a mole ratio of 1:3) in an evacuated quartz tube. The tube was heated in the furnace with a temperature gradient. The temperature of the furnace was set at 560 °C on the one side and at 600 °C on the other side. The tube was put on the furnace for several hours, where the starting material was laid on the high temperature side. The grain crystals of Ta or TaS_3 were transported to the low temperature side by convection, and grew into crystals there. After several hours, we picked up the tube and quenched its high temperature side by liquid nitrogen because this prevent sulfur adhering to the quartz tube. We obtained conventional whisker (needle-like) crystals, ring/tube crystals, and the polyhedral ring crystals.

Results

We discovered polyhedral topological crystals in MX_3 (M: transition metal, X: chalcogen), which are ring crystals having several vertices, for the first time.[22] These crystals were synthesized together with whiskers and ring crystals. Figure 2 shows typical topological crystals and polyhedral topological crystals. The whisker crystals are usually very thin with typical thicknesses of 0.1 $\sim$ 10 μm and lengths of 10 μm $\sim$ 1 cm, because of the quasi-one dimensional (1-d) crystal structure, where the basic structure of TaS_3 is triangular prism whose structure is one metallic atom

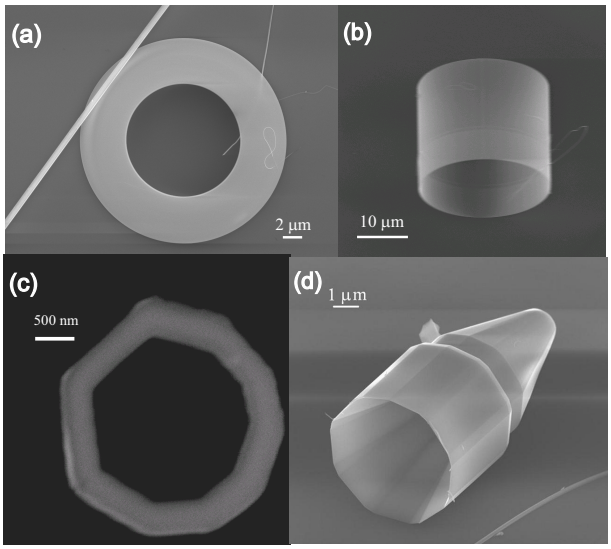

Figure 2: Topological crystals and polyhedral topological crystals of TaS_3. (a) Ring and (b) tube of smooth topological crystals. (c) Nonagon crystal and (d) Pencil-shaped of polyhedral topological crystals.

surrounded by six chalcogen atoms. The longest dimension is parallel to the axis of symmetry of triangular prism. Our samples of TaS_3 belong to the orthorhombic system.[12] The crystal of TaS_3 displays $Pmn2_1$ space group symmetry.[23] The lattice constants are referred to a = 36.804 Å, b = 15.177 Åand c = 3.340 Å. The c-axis corresponds to the longest (1-d) dimension. Ring/tube crystals, as shown in Figure 2 (a) and (b), are typical thicknesses of 0.1 $\sim$ 100 μm, width of 0.1 μm $\sim$ 10 μm and radius of 1 μm $\sim$ 100 μm. A 1-d axis is parallel to the circumference.

Shown in Figure 2 (c) and (d) are scanning electron microscopy images of typical polyhedral topological crystals we discovered. The dimensions of the polyhedral topological crystal in Figure 2 (c) are 500 nm in width, 1.8 μm in radius and 1 μm in thickness. The interior angles of each vertex are not equal. In the case of Figure 2 (c), the crystal is shaped as a nonagon, and, in the case of Figure 2 (d), the radius of the crystal becomes gradually small from 4.5 μm to 1.0 μm, like a pencil.

We investigated the orientation of crystal axes of ring crystals and polyhedral crystals as a function of position using electron backscatter diffraction patterns (EBSD) in order to confirm their crystallinity and flatness of the facets. The spatial resolution of the EBSDs is several tens of

nanometers, and this is dependent on the electron probe radius. We set up a ring (Figure 3 (a)) and a polyhedral (Figure 3 (b)) crystals. In Figure 3, the brightness in the map is proportional to intensity of EBSD.[24] Note that the high crystallinity area shows high intensity of EBSD. Figure 4 shows crystal misorientation (difference of the orientation of facets) profile of the two crystals, scanned along the green arrow. The blue line shows the variation in the orientation of crystal axis from the initial point of the green circle and red line shows that from an adjacent point. The orientation of facets changes smoothly in the ring crystal, whereas significant jumps are discretely observed at the distances of 4, 5, 7 and 9 μm in the polyhedral crystal.

Discussion

In order to make clear formation mechanism of the polyhedral structures, we investigated size distribution of 32 topological crystals of TaS_3. They included 7 polyhedral crystals and 25 ring/tube crystals. We measured their center-radius R and width W. The distribution of the topological crystals are plotted in Figure 5. Each red square represents a polyhedral ring crystal and each black circle represents a smooth ring crystal. We became aware on that the ring crystals with the radius smaller than 2 μm became the polyhedral ring crystals. This suggests that the radius must play an important role for the localization of dislocations.

We compared our results with the *R*-*W* phase diagram of ring crystals predicted by Hayashi *et*

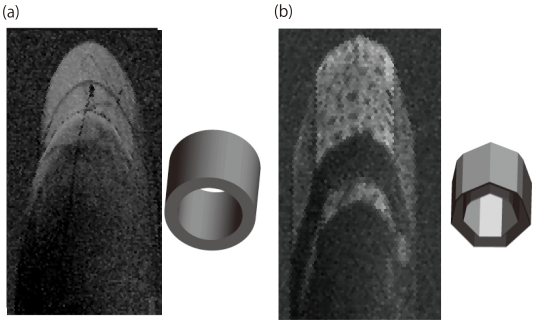

Figure 3: Intensity map of (a) a ring and (b) a polyhedral crystals of EBSD using field emission scanning electron microscope. The samples were observed from this layout.

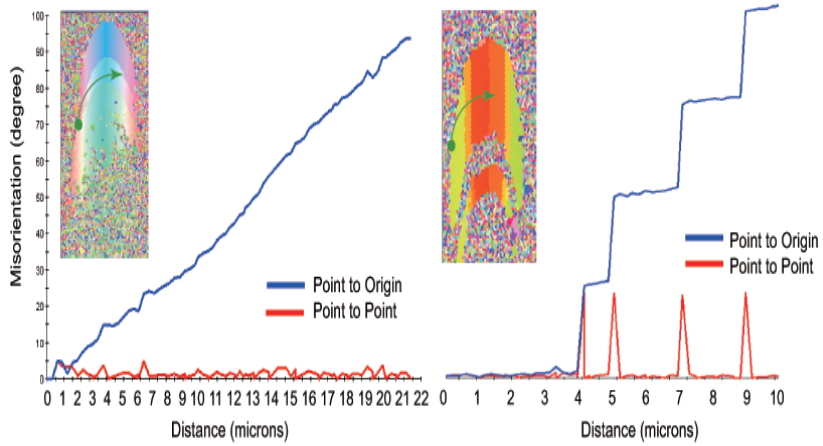

Figure 4: Misorientation profile from initial point (green circle) to green arrows. (LEFT) Ring and (RIGHT) polyhedral crystals shows, respectively. The blue line shows the variation in the orientation from the initial point of the green circle and red line shows that from an adjacent point. Insets mean that same orientation become same color.

al. who applied Ginzbrug-Landau theory for superconductivity.[21] They predicted three phases for ring crystals. In the phase I, the crystals are free from dislocation. In the phase II, the dislocations are introduced into the ring crystals to relax the bending energy. In the phase III, since the defects are too dense, there is no inter-plane rigidity. They also predicted polygonization in the phase II. In Figure 5, the phase I is colored by purple, the phase II blue and yellow, and the phase III red. The black area is the forbidden area since $R < W$. To calculate the phase boundaries, we used parameters of TaS_3 [25,26] as $\gamma^2 \simeq 10^{-2}$, d_x= 0.3 nm and d_y= 2 nm for the equations $R_{c1} = \pi W^2/2\gamma d_y$ and $R_{c2} = 2\pi d_y^2/\gamma d_x$ in the reference,[21] where γ^2 is Young's modulus divided by shear modulus, d_x is lattice constant in x-direction and d_y is that in y-direction. The boundary radius R_{c2} divided into phase III and phase II is equal to 133.3 nm, and the boundary radius R_{lim}, which is equal to the smallest R_{c1}, divided into phase II and phase I is equal to 1138 nm. The boundary R_{lim} correspond approximately to ring-tube boundary of our result. Hence, the tube crystals correspond to a clear circle without the defects. In the case of the ring crystal containing edge dislocations, the arrangement of them is nontrivial and is not confirmed. We reveal that the crystals become mostly the polyhedral crystals when the R is smaller than 2 μm in the R-W diagram. In consequence, we

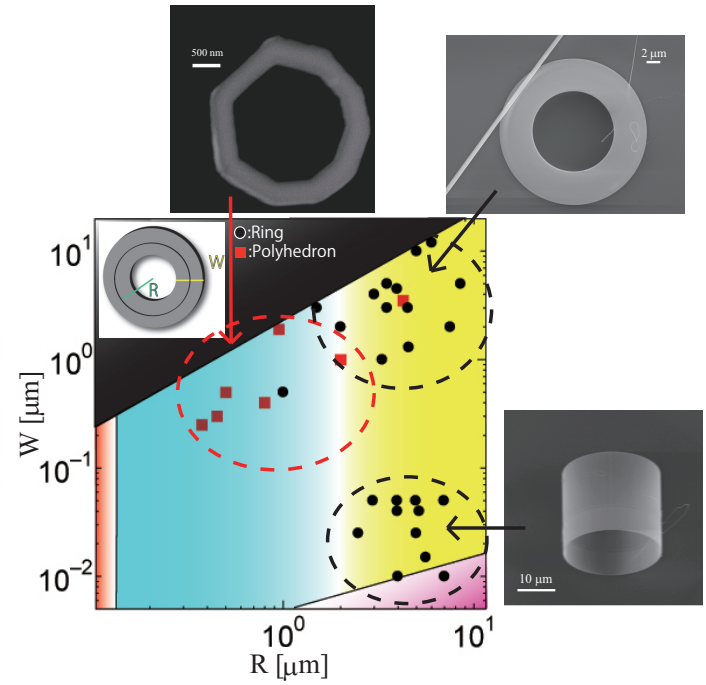

Figure 5: Phase diagram of topological crystals by the dependence of the radius and the width. The red squares mean polyhedral crystals and the black circles mean ring crystals, respectively. The black area shows the area in which ring crystal formation is forbidden. The other three areas divided by two black lines are based on Hayashi's theory. When the radius is smaller than 2 μm, the crystals become polyhedrons. The boundary between polyhedral and ring crystals is drawn by white line.

draw the boundary between the polyhedral and ring crystal areas, indicated by white line between blue and yellow areas in Figure 5. In the end, Figure 5 is divided into four areas; red, purple, blue and yellow. We discovered experimentally that the vertices are inherent in the ring crystal, and the phase transition from ring to polyhedral crystal is caused by the variation in radius size.

Our results suggest that the main factor of the polygonization is the radius-dependent interaction between the edge dislocations. Figure 6 shows the relationship between the interaction energy and the position of dislocations. The red symbols ($\perp$ symbols) represent positions of the edge dislocations, and the black curves show the interaction energy.[27] When two dislocations move on the same crystal line or plane, a repulsive force is exerted between them. As a result of the dislocation motion, plastic deformation occurs in an edge of a bulk crystal to reduce the stress within it. The passage of a dislocation through a bulk crystal is equivalent to a slip displacement of one part

of the bulk crystal. This is consistent with a bulk crystal, but, in the case of topological crystals, this model is not applicable. Topological crystals with the closed curve do not have an edge, and hence slipping dislocation cannot exit from the crystal. When many dislocations are generated, cylinder-shaped walls of dislocations are expected to be formed as a result of arrangement on parallel line.[16,17] Here, we considered two dislocations moving on different crystal lines or planes. When two dislocations were separated sufficiently far, a repulsive force is exerted, however, when the distance is short, an attractive force is exerted. As a result of the attractive interaction, the edge dislocations are concentrated in a vertical line. This is called a polygonization wall (Figure 7).[28,29] The average distance between dislocations becomes a function of *R*. Thus suppose the number of edge dislocations is constant, when the radius is large, a ring crystal is formed with a repulsive force, and when the radius is small, a polyhedral crystal is formed with an attractive force.

Since the polygonization is controlled by two parameters, our result is different from the structure of other multifaceted crystals by self-assembly[30,31] in terms of the growth mechanism. Similar polyhedral nano- and microstructures were discovered in graphite system in 2000.[32] A theoretical calculation of free energy indicated that their polygonization occurs in a graphene sheet with a diameter of less than 15 nm.[33] However, the polygonization of MX_3 topological crystals shows micrometer scale. Forming the corners from a whisker is entirely different from forming ones from a six-member carbon ring because the former configuration has a 1-d line and the latter configuration has 2-d film. The polygonization of MX_3 ring crystals must be caused by different mechanism. In context, we believe that our discovery contains the novel research field of crystallography. An amount and a position of the defects within the crystal will be confirmed by the observation of topological phenomena.

Conclusion

In summary, we discovered polyhedral topological crystals in TaS_3 system. Formation mechanism is related to the edge dislocations arrayed on vertical line by the distance-dependent interaction

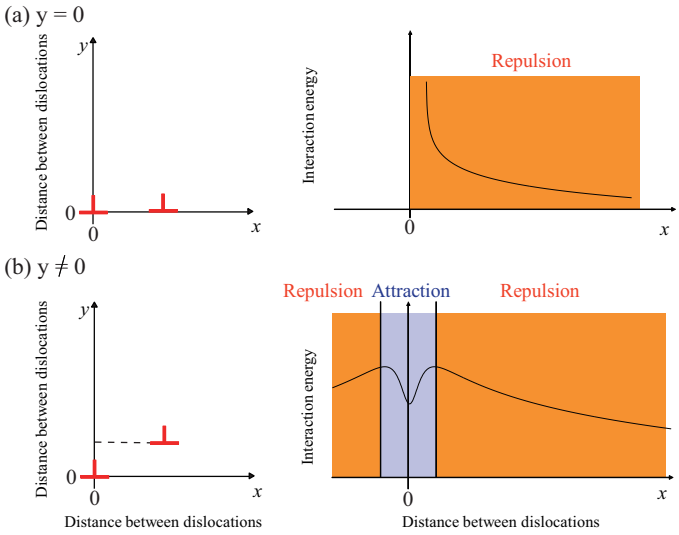

Figure 6: Interaction energy between the edge dislocations on (a) the same plane and (b) other planes shifting to vertical (y-) direction. The red symbols ($\perp$ symbols) and the black lines show the edge dislocations and interaction energy in x-direction. In a large distance, a repulsive force is exerted, and in a short distance, an attractive force is exerted in the case of (b).

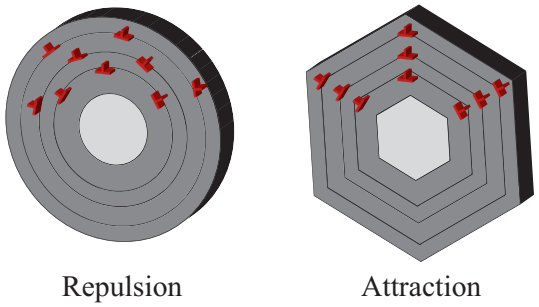

Figure 7: Polygonization walls as a result of concentration of the edge dislocations on vertical line.

between them. We proposed a polygonization phase in the width versus radius phase diagram for ring-shaped crystals.

Acknowledgement

The authors are grateful to T. Toshima, T. Tsuneta, K. Ichimura, and K. Yamaya, for experimental support and M. Hayashi, N. Hatakenaka for stimulating discussions. This research has been supported by Grant-in-Aid for the 21st Century COE program on "Topological Science and Technology" and the Japan Society for the Promotion of Science.

References

(1) Kroto, H. W.; Heath, J. R.; O'Brien, S. C.; Curl, R. F.; Smalley, R. E. *Nature* **1985**, *318*, 162-163.

(2) Tenne, R.; Margulis, L.; Genut, M.; Godes, G. *Nature* **1992**, *360*, 444-446.

(3) Iijima, S. *Nature* **1991**, *354*, 56-58.

(4) Aharonov, Y.; Bohm, D. *Phys. Rev.* **1959**, *115*, 485-491.

(5) Bong, D. T.; Clark, T. D.; Granja, J. R.; Ghadiri, M. R. *Angew. Chem., Int. Ed.* **2001**, *40*, 988-1011.

(6) Zhou, L.; Wang, W.; Zhang, L.; Xu, H.; Zhu, W. *J. Phys. Chem. C* **2007**, *111*,13659-13664.

(7) Hosten, O.; Kwiat, P. *Science* **2008**, *319*, 787-790.

(8) Tanda, S.; Kawamoto, H.; Shiobara, M.; Sakai, Y.; Yasuzuka, S.; Okajima, Y. *Physica B* **2000**, *284*, 1657-1658.

(9) Tanda, S.; Tsuneta, T.; Okajima, Y.; Inagaki, K.; Yamaya, K.; Hatakenaka, N. *Nature* **2002**, *417*, 397-398.

(10) Matsuura, T.; Yamanaka, M.; Hatakenaka, N.; Matsuyama, T.; Tanda, S. *J. Crys. Grow.* **2006**, *297*, 157-160.

(11) Matsuura, T.; Tanda, S.; Asada, K.; Sakai, Y.; Tsuneta, T.; Inagaki, K.; Yamaya, K. *Physica B* **2003**, *329*, 1550-1551.

(12) Tsubota, M.; Inagaki, K.; Tanda, S. *Physica B* **2009**, *404*, 416-418.

(13) Nobukane, H. *private communication*.

(14) Shimatake, K.; Toda, Y.; Tanda, S. *Phys. Rev. B* **2006**, *73*, 153403-1-153403-4.

(15) Matsuura, T.; Tsuneta, T.; Inagaki, K.; Tanda, S. *Phys. Rev. B* **2006**, *73*, 165118-1-165118-5.

(16) Tsuneta, T.; Yamamoto, K.; Ikeda, N.; Nogami, Y.; Matsuura, T.; Tanda, S. *Phys. Rev. B* **2010**, *82*, 014105-1-014105-6.

(17) Matsuura, T.; Tsuneta, T.; Kumagai, G.; Tsubota, M.; Matsuyama, T.; Tanda, S. *Phys. Rev. B* **2011**, *83*, 174113-1-174113-5.

(18) Taylor, G. I. *Proc. Roy. Soc. A* **1934**, *145*, 362-405.

(19) Polanyi, M. *Z. Physik* **1934**, *89*, 660-664.

(20) Orowan, E. *Z. Physik* **1934**, *89*, 605-634.

(21) Hayashi, M.; Ebisawa, H.; Kuboki, K. *Euro. Phys. Lett.* **2006**, *76(2)*, 264-270.

(22) Tsubota, M.; Toshima, T.; Hara, J.; Kumagai, G.; Hanzawa, H.; Ichimura, K.; Tanda, S. *Acta Crystallographica Sec. A supplement* **2008**, *64*, C509.

(23) Kagoshima, S.; Nagasawa, H.; Sambongi, T. *One-Dimensional Conductors* (Springer-Verlag, Berlin, 1988).

(24) Schwartz, A. J.; Kumar, M.; Adams, B. L. *Electron Backscatter Diffraction in Materials Science* (Kluwer Academic/Plenum Publishers, New York, 2000).

(25) Xiang, X. D.; Brill, J. W. *Phys. Rev. B* **1987**, *36*, 2969-2971.

(26) Yamaya, K.; Oomi, G. *J. Phys. Soc. Jpn.* **1982**, *51*, 3512-3515.

(27) Read, W. T.; Jr. *Dislocations in Crystals*, 3rd ed. (McGraw-Hill, 1953).

(28) Cottrell, A. H. *Dislocations and Plastic Flow in Crystals*, (Oxfold, 1953).

(29) Mott, N. F. *Proc. R. Soc. Ser. B* **1951**, *64*, 729-741.

(30) Medina, D. D.; Mastai, Y. *Cryst. Growth Des.* **2008**, *8*, 3646-3651.

(31) Pérez-Hernández, N.; Fort, D.; Pérez, C.; Martín, J. D. *Cryst. Growth Des.* **2011**, *11(4)*, 1054-1061.

(32) Gogotsi, Y.; Libera, J. A.; Kalashnikov, N.; Yoshimura, M. *Science* **2000**, *290*, 317-320.

(33) Speck, J. S.; Endo, M.; Dresselhaus, M. S. *J. Crys. Grow.* **1989**, *94*, 834-848.